4. THE DENSITY MATRIX DESCRIPTION OF A DOUBLE-QUANTUM COHERENCE EXPERIMENT (INADEQUATE)

The main goal of INADEQUATE (**I**ncredible **N**atural **A**bundance **D**oubl**E** **QUA**ntum **T**ransfer **E**xperiment) is to eliminate the strong signal of noncoupled ^{13}C nuclei in order to easily observe the 200 times weaker satellites due to C-C coupling. This is realized by exploiting the different phase responses of the coupled and non-coupled spin signals when the phase of the observe pulse is varied (see Figure I.7). The receiver phase is matched with the desired signal. It shall be seen that the different phase behavior of the coupled nuclei is connected with their double-quantum coherence. The beauty of INADEQUATE resides in its basic simplicity: only a two-step cycle is theoretically needed to eliminate the unwanted signal. That the real life sequences may reach 128 or more steps is exclusively due to hardware (pulse) imperfections whose effects must be corrected by additional phase cycling.

The essence of INADEQUATE can be understood by following the basic sequence shown in Figure I.7.

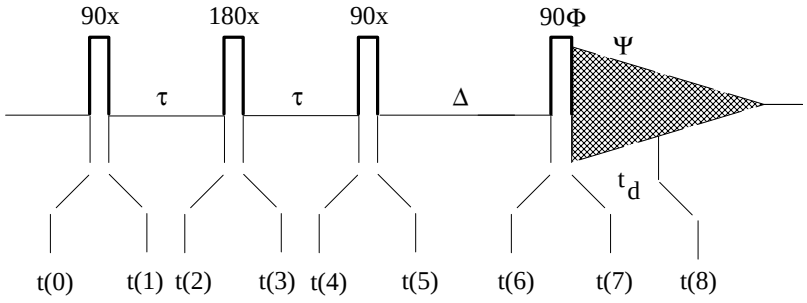

Figure I.7. The INADEQUATE sequence: $90x - \tau - 180x - \tau - 90x - \Delta - 90\Phi - AT$ (proton decoupling is applied throughout the experiment).

4.1 Equilibrium Populations

At thermal equilibrium the four energy levels shown in Figure I.8 are populated according to the Boltzmann distribution law, as shown in (I.1) through (I.5). In this case both ν_A and ν_X are ^{13}C transition frequencies. The difference between ν_A and ν_X, due to different chemical shifts, is too small to be taken into account when calculating the populations. We assume $q = p$ and (I.6) becomes:

$$\begin{aligned} P_1 &= P_1 \\ P_2 &= (1+p)P_1 \\ P_3 &= (1+p)P_1 \\ P_4 &= (1+2p)/P_1 \end{aligned}$$

$$1 = (4+4p)P_1 = P_1 S$$

Hence,

$$\begin{aligned} P_1 &= 1/S \\ P_2 = P_3 &= (1+p)/S \\ P_4 &= (1+2p)/S \end{aligned}$$

where

$$S = 4 + 4p \cong 4$$

and the density matrix at equilibrium is:

$$D(0) = \begin{bmatrix} P_1 & 0 & 0 & 0 \\ 0 & P_2 & 0 & 0 \\ 0 & 0 & P_3 & 0 \\ 0 & 0 & 0 & P_4 \end{bmatrix} = \frac{1}{4}\begin{bmatrix} 1 & 0 & 0 & 0 \\ 0 & 1+p & 0 & 0 \\ 0 & 0 & 1+p & 0 \\ 0 & 0 & 0 & 1+2p \end{bmatrix}$$

$$= \frac{1}{4}\begin{bmatrix} 1 & 0 & 0 & 0 \\ 0 & 1 & 0 & 0 \\ 0 & 0 & 1 & 0 \\ 0 & 0 & 0 & 1 \end{bmatrix} + \frac{p}{4}\begin{bmatrix} 0 & 0 & 0 & 0 \\ 0 & 1 & 0 & 0 \\ 0 & 0 & 1 & 0 \\ 0 & 0 & 0 & 2 \end{bmatrix} \qquad \text{(I.60)}$$

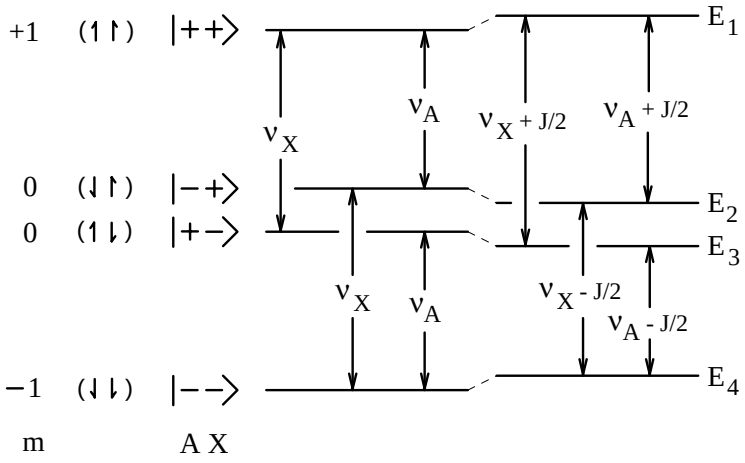

Figure I.8. Energy levels of a homonuclear AX system (noncoupled and coupled). Transition frequencies and coupling constants are in Hz.

We will again ignore the (large) first term which is not affected by pulses or evolution, put aside the constant factor $p/4$ and start with

$$D(0) = \begin{bmatrix} 0 & 0 & 0 & 0 \\ 0 & 1 & 0 & 0 \\ 0 & 0 & 1 & 0 \\ 0 & 0 & 0 & 2 \end{bmatrix} \tag{I.61}$$

In order to compare the results of the density matrix treatment with those of the vectorial representation, we will calculate for every step of the sequence the magnetization components, using the relations (B15) − (B22). We must also consider that here $q = p$ and that $M_{oA} = M_{oX} = M_o/2$, where M_o refers to magnetization due to adjacent ^{13}C atoms A and X. Thus our magnetization equations become (cf. I.53):

$$\begin{aligned} M_{zA} &= -(M_o/4)(d_{11} - d_{22} + d_{33} - d_{44}) \\ M_{zX} &= -(M_o/4)(d_{11} - d_{33} + d_{22} - d_{44}) \\ M_{TA} &= -(M_o/2)(d^*_{12} + d^*_{34}) \\ M_{TX} &= -(M_o/2)(d^*_{13} + d^*_{24}) \end{aligned} \tag{I.62}$$

One can check that at thermal equilibrium, when $D = D(0)$

$$M_{zA} = -(M_o/4)(0-1+1-2) = M_o/2$$
$$M_{zX} = -(M_o/4)(0-1+1-2) = M_o/2$$

The transverse magnetization

$$M_{TA} = M_{TX} = 0$$

4.2 The First Pulse

At time $t(0)$ a nonselective pulse $90xAX$ is applied. Since all pulses in this sequence are nonselective, the notation AX will be omitted. The density matrix $D(1)$ after the pulse is calculated according to:

$$D(0) = R^{-1}D(0)R$$

The rotation operator R and its reciprocal R^{-1} for the nonselective $90x$ pulse have been calculated in (I.34):

$$R = \frac{1}{2}\begin{bmatrix} 1 & i & i & -1 \\ i & 1 & -1 & i \\ i & -1 & 1 & i \\ -1 & i & i & 1 \end{bmatrix} \quad ; \quad R^{-1} = \frac{1}{2}\begin{bmatrix} 1 & -i & -i & -1 \\ -i & 1 & -1 & -i \\ -i & -1 & 1 & -i \\ -1 & -i & -i & 1 \end{bmatrix}$$

First we postmultiply D(0) by R:

$$D(0)R = \begin{bmatrix} 0 & 0 & 0 & 0 \\ i & 1 & -1 & i \\ i & -1 & 1 & i \\ -2 & 2i & 2i & 2 \end{bmatrix}$$

Premultiplication with R^{-1} leads to

$$D(1)=\frac{1}{4}\begin{bmatrix} 4 & -2i & -2i & 0 \\ 2i & 4 & 0 & -2i \\ 2i & 0 & 4 & -2i \\ 0 & 2i & 2i & 4 \end{bmatrix}=\frac{1}{2}\begin{bmatrix} 2 & -i & -i & 0 \\ i & 2 & 0 & -i \\ i & 0 & 2 & -i \\ 0 & i & i & 2 \end{bmatrix} \qquad \text{(I.63)}$$

We note that the 90° pulse equalizes the populations and creates single-quantum coherences. The longitudinal magnetization is null while

$$M_{TA}=-(M_o/2)(i/1+i/2)=-iM_o/2$$
$$M_{TX}=-(M_o/2)(i/1+i/2)=-iM_o/2$$
$$M_T=M_{TA}+M_{TX}=-iM_o$$

We also note that the transverse magnetization is imaginary. Considering that $M_T = M_x + iM_y$, it follows that $M_x = 0$ and $M_y = -M_o$.

So far, the vector representation would have been much simpler to use. Let us see, though, what happens as we proceed.

4.3 Evolution from *t* (1) to *t* (2)

The standard formula describing the (laboratory frame) time evolution of the density matrix elements in the absence of a pulse is:

$$d_{mn}(t)=d_{mn}(0)\exp(-i\omega_{mn}t) \qquad \text{(I.64)}$$

d_{mn} is the matrix element and $\omega_{mn} = (E_m - E_n)/\hbar$ is the angular frequency of transition $m \rightarrow n$. Note that $d_{mn}(0)$ is the starting point of the evolution immediately after a given pulse. In our case the elements $d_{mn}(0)$ are those of $D(1)$. If the evolution is described in a frame rotating at transmitter frequency ω_{tr} equation (I.64) becomes:

$$d_{mn}(t)=d_{mn}(0)\exp(-i\omega_{mn}t)\exp[i(m_m-m_n)\omega_{tr}t] \qquad \text{(I.65)}$$

where m_m and m_n are the total magnetic quantum numbers of states *m* and *n* (see Appendix B).

Let us apply (I.65) to our particular case ($m_1 = 1$; $m_2 = m_3 = 0$; $m_4 = -1$). As expected, the diagonal elements are invariant during evolution since both exponentials are equal to 1. All single quantum coherences above diagonal have $m_m - m_n = 1$. Hence,

$$\begin{aligned} d_{mn}(t) &= d_{mn}(0)\exp(-i\omega_{mn}t)\exp(i\omega_{tr}t) \\ &= d_{mn}(0)\exp[-i(\omega_{mn}-\omega_{tr})t] \\ &= d_{mn}(0)\exp(-i\Omega_{mn}t) \end{aligned} \tag{I.66}$$

where Ω_{mn} is the evolution frequency in the rotating frame.

The rotating frame treatment is useful not only for better visualization of the vector evolution but, also, because the detection is actually made at the resulting low (audio) frequencies.

For the double-quantum coherence matrix element

$$\begin{aligned} d_{14}(t) &= d_{14}(0)\exp(-i\omega_{14}t)\exp[i(1+1)\omega_{tr}t] \\ &= d_{14}(0)\exp(-i\Omega_{14}t) \end{aligned} \tag{I.67}$$

where $\Omega_{14} = \omega_{14} - 2\omega_{tr}$. We note that both single- and double-quantum coherences evolve at low frequencies in the rotating frame.

The zero-quantum coherence matrix element is not affected by the rotating frame ($m_2 - m_3 = 0$):

$$d_{23}(t) = d_{23}(0)\exp(-i\omega_{23}t) = d_{23}(0)\exp(-i\Omega_{23}t) \tag{I.68}$$

The zero-quantum coherence evolves at low frequency in both the laboratory and rotating frame.

We now want to calculate $D(2)$, i.e., the evoluition during the first delay τ. For instance

$$d_{12}(2) = d_{12}(1)\exp(-i\Omega_{12}\tau) = -(-i/2)\exp(-i\Omega_{12}\tau) \tag{I.69}$$

To save space we let $(-i/2)\exp(-i\Omega_{mn}\tau) = B_{mn}$ and at $t(2)$ we have:

$$D(2) = \begin{bmatrix} 1 & B_{12} & B_{13} & 0 \\ B_{12}^{*} & 1 & 0 & B_{24} \\ B_{13}^{*} & 0 & 1 & B_{34} \\ 0 & B_{24}^{*} & B_{34}^{*} & 1 \end{bmatrix} \tag{I.70}$$

The *z*-magnetization is still zero (relaxation effects are neglected). The transverse magnetization components are:

$$\begin{aligned} M_{TA} &= -(M_o/2)(B_{12}^* + B_{34}^*) \\ &= -(iM_o/4)[\exp(i\Omega_{12}\tau) + \exp(i\Omega_{34}\tau)] \end{aligned} \quad \text{(I.71)}$$

$$\begin{aligned} M_{TX} &= -(M_o/2)(B_{13}^* + B_{24}^*) \\ &= -(iM_o/4)[\exp(i\Omega_{13}\tau) + \exp(i\Omega_{24}\tau)] \end{aligned} \quad \text{(I.72)}$$

We see that there are four vectors rotating with four different angular velocities in the equatorial (xy) plane. We can identify (see Figure I.8):

$$\begin{aligned} \Omega_{12} &= \omega_{12} - \omega_{tr} = \Omega_A + \pi J \\ \Omega_{34} &= \Omega_A - \pi J \\ \Omega_{13} &= \Omega_X + \pi J \\ \Omega_{24} &= \Omega_X - \pi J \end{aligned}$$

4.4 The Second Pulse

The rotation operator for this pulse is

$$R_{180\,yAX} = \begin{bmatrix} 0 & 0 & 0 & 1 \\ 0 & 0 & -1 & 0 \\ 0 & -1 & 0 & 0 \\ 1 & 0 & 0 & 0 \end{bmatrix} = R_{180\,yAX}^{-1} \quad \text{(I.73)}$$

At time *t*(3) the density matrix is:

$$D(3) = R^{-1}D(2)R = \begin{bmatrix} 1 & -B_{34}^* & -B_{24}^* & 0 \\ -B_{34} & 1 & 0 & -B_{13}^* \\ -B_{24} & 0 & 1 & -B_{12}^* \\ 0 & -B_{13} & -B_{12} & 1 \end{bmatrix} \quad \text{(I.74)}$$

Two important changes have been induced by the 180° pulse. First, all single quantum coherences were conjugated and changed sign.

This means that all *x*-components changed sign while the *y*-components remained unchanged:

$$M_T = M_x + iM_y$$
$$-M_T^* = -M_x + iM_y$$

This shows, indeed, that all four vectors rotated 180° around the *y*-axis. Second, coherences corresponding to fast precessing nuclei were transferred in "slots" corresponding to slow evolution. This means the vectors also changed labels.

4.5 Evolution from *t* (3) to *t* (4)

According to (I.66) and (I.74), the evolution during the second τ delay leads to

$$\begin{aligned} d_{12}(4) &= d_{12}(3)\exp(-i\Omega_{12}\tau) = B_{34}^*\exp(-i\Omega_{12}\tau) \\ &= (-i/2)\exp(+i\Omega_{34}\tau)\exp(-i\Omega_{12}\tau) \\ &= (-i/2)\exp[-i(\Omega_{12}-\Omega_{34})\tau] = (-i/2)\exp(-i2\pi J\tau) \end{aligned} \quad \text{(I.75)}$$

$$d_{13}(4) = (-i/2)\exp(-i2\pi J\tau) = d_{12}(4) = U \quad \text{(I.76)}$$

$$d_{24}(4) = d_{34}(4) = (-i/2)\exp(+i2\pi J\tau) = V \quad \text{(I.77)}$$

Hence,

$$D(4) = \begin{bmatrix} 1 & U & U & 0 \\ U^* & 1 & 0 & V \\ U^* & 0 & 1 & V \\ 0 & V^* & V^* & 1 \end{bmatrix} \quad \text{(I.78)}$$

Using (I.62) we calculate the corresponding magnetization vectors:

$$M_{zA} = M_{zX} = 0$$
$$M_{TA} = M_{TX} = -M_o(U^* + V^*) = -iM_o\cos 2\pi J\tau \quad \text{(I.79)}$$

We see that while the chemical shifts refocused the coupling continues to be expressed, due to the label change.

4.6 The Third Pulse

We apply to $D(4)$ the same rotation operators we used for the first pulse and we obtain:

$$D(5) = \begin{bmatrix} 1+c & 0 & 0 & -is \\ 0 & 1 & 0 & 0 \\ 0 & 0 & 1 & 0 \\ is & 0 & 0 & 1-c \end{bmatrix} \qquad \text{(I.80)}$$

where $c = \cos 2\pi J\tau$ and $s = \sin 2\pi J\tau$.

$D(5)$ tells us that all single-quantum coherences vanished, a double-quantum coherence was created and the only existing magnetization is along the z-axis. Turning to vector representation, it is seen that before the pulse [see(I.78)] we had magnetization components on both x and y axes, since U and V are complex quantities. The vector description would indicate that the 90x pulse leaves the x components unchanged. In reality, as seen from the DM treatment, this does not happen since all transverse components vanish.

4.7 Evolution from *t* (5) to *t* (6)

The double-quantum coherence element, $-is$, evolves according to (I.67):

$$D(6) = \begin{bmatrix} 1+c & 0 & 0 & w \\ 0 & 1 & 0 & 0 \\ 0 & 0 & 1 & 0 \\ w^* & 0 & 0 & 1-c \end{bmatrix} \qquad \text{(I.81)}$$

where $w = -is\exp(-i\Omega_{14}\Delta) = -i\sin 2\pi J\tau \exp(-i\Omega_{14}\Delta)$.

Our interest is in the double-quantum coherence w. In order to maximize it, we select $\tau = (2k+1)/4J$ where k = integer. Then $c = 0$ and $s = \sin[(2k+1)\pi/2] = \pm 1 = (-1)^k$

With this value of τ.

$$D(6) = \begin{bmatrix} 1 & 0 & 0 & w \\ 0 & 1 & 0 & 0 \\ 0 & 0 & 1 & 0 \\ w^* & 0 & 0 & 1 \end{bmatrix} \tag{I.82}$$

where $w = -i(-1)^k \exp(i\Omega_{14}\Delta)$

The last expression of $D(6)$ tells us that at this stage there is no magnetization at all in any of the three axes. This would be impossible to derive from the vector representation, which also could not explain the reapparition of the observable magnetization components after the fourth pulse.

4.8 The Fourth Pulse

This pulse is phase cycled, i.e., it is applied successively in various combinations along the x, y, $-x$, and $-y$ axes. The general expression of the $90\Phi AX$ operator is given in Appendix C [see(C39)].

$$R_{90\Phi AX} = \frac{1}{2}\begin{bmatrix} 1 & a & a & a^2 \\ -a^* & 1 & -1 & a \\ -a^* & -1 & 1 & a \\ a^{*2} & -a^* & -a^* & 1 \end{bmatrix} \tag{I.83}$$

where $a = i\exp(-i\Phi)$ and Φ is the angle between the x-axis and the direction of B_1. When Φ takes the value 0, 90°, 180° or 270°, the pulse is applied on axis x, y, $-x$, or $-y$, respectively.

For clarity we will discuss the *coupled* and the *noncoupled (isolated)* carbon situations separately. In the first case (coupled ^{13}C spins), we observe that at $t(6)$ [see(I.82)] the populations are equalized and all information is contained in the w elements.

The result of $R^{-1}_{90\Phi AX} D(6) R_{90\Phi AX}$ is:

$$D(7) = \begin{bmatrix} 1+a^2F & -a^*G & -a^*G & F \\ aG & 1-a^2F & -a^2F & a^*G \\ aG & -a^2F & 1-a^2F & a^*G \\ F & -aG & -aG & 1+a^2F \end{bmatrix} \qquad \text{(I.84)}$$

where
$$F = (w + w^*)/4 = -(1/2)(-1)^k \sin\Omega_{14}\Delta \qquad \text{(I.85)}$$
$$G = (w - w^*)/4 = -(1/2)(-1)^k \cos\Omega_{14}\Delta$$

$D(7)$ shows that the newly created single quantum coherences contain the double quantum coherence information, Ω_{14}. The transverse magnetization is zero (fast and slow vectors are equal and opposite). A longitudinal magnetization proportional to $\sin\Omega_{14}$ appears. None of these could be deduced from the vector representation. Yet, the density matrix would allow the reader to draw the corresponding vectors.

To save time and space we will treat the isolated (uncoupled) carbons as an AX system in which A and X belong to two different molecules. We can use (I.81) letting $J = 0$ ($c = 1$; $s = 0$; $w = 0$) :

$$D'(6) = \begin{bmatrix} 2 & 0 & 0 & 0 \\ 0 & 1 & 0 & 0 \\ 0 & 0 & 1 & 0 \\ 0 & 0 & 0 & 0 \end{bmatrix} \qquad \text{(I.86)}$$

In this case $D(7)$ becomes

$$D'(7) = \begin{bmatrix} 1 & a/2 & a/2 & 0 \\ a^*/2 & 1 & 0 & a/2 \\ a^*/2 & 0 & 1 & a/2 \\ 0 & a^*/2 & a^*/2 & 1 \end{bmatrix} \qquad \text{(I.87)}$$

$D'(7)$ shows only single quantum coherences and equalized populations. The transverse magnetization of the noncoupled spins is equal to their equilibrium magnetization M'_o (its orientation depends on the value of Φ).

4.9 Detection

The magnetization at *t*(8), due to coupled (cpl) and noncoupled (ncpl) nuclei can be calculated starting from the single quantum coherences in (I.84) and (I.87) respectively.

$$M_T(cpl) = M[\exp(i\Omega_{12}t_d) + \exp(i\Omega_{13}t_d) - \exp(i\Omega_{24}t_d) - \exp(i\Omega_{34}t_d)] \qquad \text{(I.88)}$$

where $M = -M_o aG^* = (M_0/2)\exp(-i\Phi)(-1)^k \cos\Omega_{14}\Delta$

These are the four peaks of the coupled AX system shown as a schematic contour plot in Figure I.9.

For the noncoupled carbons

$$M_T(ncpl) = M'[2\exp(i\Omega_A t_d) + 2\exp(i\Omega_X t_d)] \qquad \text{(I.89)}$$

where $M' = -M_o' a^*/2 = (-iM_o'/2)\exp(-i\Phi)$

These are the two peaks of the uncoupled nuclei. Each of them is 200 times more intense than each of the four peaks in (I.88).

The culminating point of INADEQUATE is the selective detection of $M_T(cpl)$. We note that $M_T(cpl)$ and $M_T(ncpl)$ depend in opposite ways on Φ since one contains a and the other a^* [cf.(I.88) and (I.89)]. They can be discriminated by cycling Φ and properly choosing the receiver phase Ψ [the detected signal $S = M_T \exp(-i\Psi)$]. The table below shows that two cycles are sufficient to eliminate $M_T(ncpl)$.

Cycle	Φ	Ψ	ncpl ---------- exp*i*(Φ-Ψ)	cpl ---------- exp*i*(-Φ-Ψ)
1	0	0	1	1
2	90°	-90°	-1	1
(1+2)			0	2

Even small imperfections of the rf pulse will allow leakage of the strong undesired signal into the resultant spectrum. This makes it necessary to apply one of several cycling patterns consisting of up to

256 steps, which attempt to cancel the effects of too long, too short, or incorrectly phased, pulses.

4.10 Carbon-Carbon Connectivity

A significant extension of INADEQUATE is its adaptation for two-dimensional experiments. The second time-domain (in addition to t_d) is created by making Δ variable. All we have to do now is to discuss (I.88) and (I.89) in terms of two time variables.

As seen in Figure I.9, all four peaks of $M\tau(cpl)$ will be aligned in domain Δ along the same frequency $\Omega_{14} = \Omega_A + \Omega_X$. The great advantage of the 2D display consists of the fact that every pair of coupled carbons will exhibit its pair of doublets along its own Ω_{14} frequency. This allows us to trace out the carbon skeleton of an organic molecule.

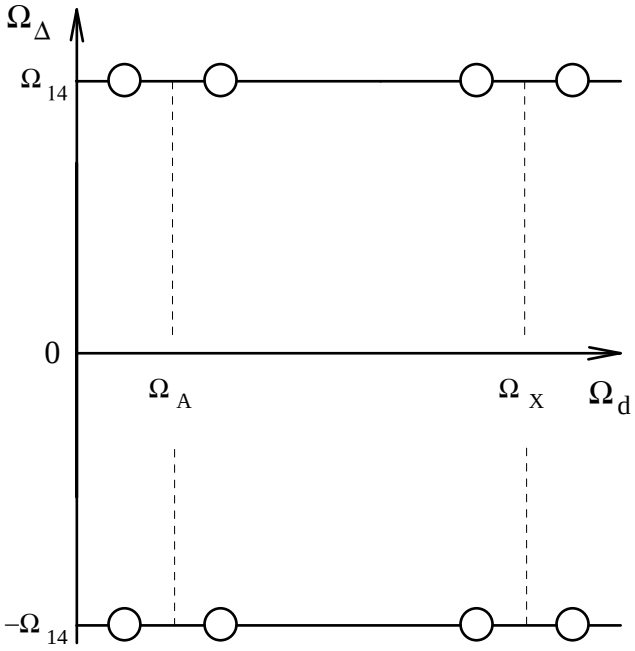

Figure I.9. The four peaks due to a pair of coupled ^{13}C atoms. The vertical scale is twice larger than the horizontal scale.

The student is invited to identify the molecule whose 2D spectrum is shown in Figure I.10 and to determine its carbon-carbon connectivities. The answer is in the footnote on page 59.

It should be noted that $M_T(ncpl)$ does not depend on Δ [cf.(I.81)]. This means that, when incompletely eliminated, the peaks of isolated carbons will be "axial" (dotted circles on the zero frequency line of domain Δ).

We also note that $M_T(cpl)$ is phase modulated with respect to t_d and amplitude modulated with respect to Δ. Consequently, mirror-image peaks will appear at frequencies $-\Omega_{14}$. This reduces the intensity of the displayed signals and imposes restrictions on the choice of the transmitter frequency, increasing the size of the data matrix. A modified sequence has been proposed to obtain phase modulation with respect to Δ, the analog of a quadrature detection in domain Δ.

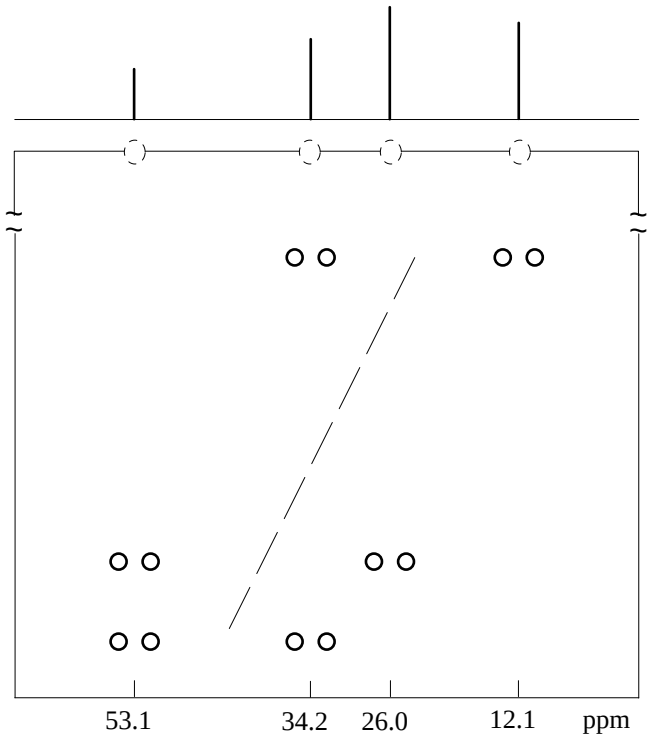

Figure I.10. The carbon-carbon connectivity spectrum of a mo-lecule with MW = 137.